Acta Biomaterialia 78 (2018) 111–122

Contents lists available at ScienceDirect

Acta Biomaterialia

journal homepage: www.elsevier.com/locate/actabiomat

Full length article

Solution fibre spinning technique for the fabrication of tuneable decellularised matrix-laden fibres and fibrous micromembranes

Zhaoying Li [a,b], Jack Tuffin [c], Iek M. Lei [a,b], Francesco S. Ruggeri [d], Natasha S. Lewis [a,b], Elisabeth L. Gill [a,b], Thierry Savin [a], Luai Huleihel [e], Stephen F. Badylak [e], Tuomas Knowles [d,f], Simon C. Satchell [c], Gavin I. Welsh [c], Moin A. Saleem [c], Yan Yan Shery Huang [a,b,*]

[a] Department of Engineering, University of Cambridge, Cambridge CB2 1PZ, UK
[b] The Nanoscience Centre, University of Cambridge, Cambridge CB3 0FF, UK
[c] Bristol Medical School: Translational Health Sciences, University of Bristol, Bristol BS1 3NY, UK
[d] Department of Chemistry, University of Cambridge, Cambridge CB2 1EW, UK
[e] McGowan Institute for Regenerative Medicine, Pittsburgh, PA 15219, USA
[f] Cavendish Laboratory, University of Cambridge, Cambridge, CB3 1HE, UK

ARTICLE INFO

Article history:
Received 1 March 2018
Received in revised form 5 August 2018
Accepted 7 August 2018
Available online 10 August 2018

Keywords:
Extracellular matrix
Electrospinning
Fibre
Membrane stiffness
In vitro models

ABSTRACT

Recreating tissue-specific microenvironments of the extracellular matrix (ECM) *in vitro* is of broad interest for the fields of tissue engineering and organ-on-a-chip. Here, we present biofunctional ECM protein fibres and suspended membranes, with tuneable biochemical, mechanical and topographical properties. This soft and entirely biologic membrane scaffold, formed by micro-nano-fibres using low voltage electrospinning, displays three unique characteristics for potential cell culture applications: high-content of key ECM proteins, single-layered mesh membrane, and flexibility for *in situ* integration into a range of device setups. Extracellular matrix (ECM) powder derived from urinary bladder, was used to fabricate the ECM-laden fibres and membranes. The highest ECM concentration in the dry protein fibre was 50 wt%, with the rest consisting of gelatin. Key ECM proteins, including collagen IV, laminin, and fibronectin, were shown to be preserved post the biofabrication process. The single fibre tensile Young's modulus can be tuned for over two orders of magnitude between ~600 kPa and 50 MPa depending on the ECM content. Combining the fibre mesh printing with 3D printed or microfabricated structures, culture devices were constructed for endothelial layer formation, and a trans-membrane co-culture formed by glomerular cell types of podocytes and glomerular endothelial cells, demonstrating feasibility of the membrane culture. Our cell culture observation points to the importance of membrane mechanical property and re-modelling ability as a factor for soft membrane-based cell cultures. The ECM-laden fibres and membranes presented here would see potential applications in *in vitro* assays, and tailoring structure and biological functions of tissue engineering scaffolds.

Statement of Significance

Recreating tissue-specific microenvironments of the extracellular matrix (ECM) is of broad interest for the fields of tissue engineering and organ-on-a-chip. Both the biochemical and biophysical signatures of the engineered ECM interplay to affect cell response. Currently, there are limited biomaterials processing methods which allow to design ECM membrane properties flexibly and rapidly. Solvents and additives used in many existing processes also induced unwanted ECM protein degradation and toxic residues. This paper presents a solution fibre spinning technique, where careful selection of the solution combination led to well-preserved ECM proteins with tuneable composition. This technique also provides a highly versatile approach to fabricate ECM fibres and membranes, leading to designable fibre Young's modulus for over two orders of magnitude.

* Corresponding author at: Department of Engineering, University of Cambridge, Cambridge CB2 1PZ, UK.
E-mail address: yysh2@cam.ac.uk (Y.Y.S. Huang).

https://doi.org/10.1016/j.actbio.2018.08.010
1742-7061/

1. Introduction

The microstructures and compositions of extracellular matrices (ECMs) are complex and organ-specific [1]. In recent years, there have been tremendous interests in replicating the multi-faceted and multi-component ECM cues *in vitro*, for better understanding of stem cell maintenance and differentiation, or for creating functional tissue replacements. Recent progress in decellularised matrix derived from harvested tissues and organs shows the possibility of retaining most biochemical ingredients of the physiological ECM, whilst eliminating previous resident cellular components [2–4]. The efficacy and ease of decellularisation comes at the expense of the preservation of ECM ultrastructure [5]. For instance, whole organ perfusion-decellularisation presents a protocol that least disrupts the pristine ECM ultrastructure [4]. Although this method shows promising applications for xenogeneic transplantation and tissue engineering [6], it may have restricted scope for applications such as *in vitro* experiments, micro-device integration, and personalised scaffold manufacturing. In comparison, mechanical abrasion and freeze-thaw process provide effective decellularisation with the benefits of high throughput, large-scale, and the ease of product preservation. This process gives rise to homogenised ECM materials, which are reduced to the forms of powder and hydrogel, and have been employed in a number of 2D and 3D cell culture studies [7,8].

To harness the readily available homogenised ECM sources, ongoing development can lie in advancing biofabrication techniques that tailor the topography, mechanical property and ultrastructures of fibrous scaffolds, while optimally retaining the ECM biochemical components. Considering that the native ECM proteins contain defined structural building blocks of nano-microfibres, here, we explored the fabrication of ECM-laden fibres, with diameters in the hundreds of nanometres to micrometre range. Although prior studies have reported the production of ECM-incorporated composite fibres (mainly based on far-field electrospinning techniques), the content of ECM within the fibre is generally low with respect to the bulk fibre (i.e. estimated 0.45 wt% [9] and ~1 wt% [10]). Another technical challenge lies in the dilemma for fabricating robust scaffolds for device integration, against the needs for soft interfacing matrices. Within these, suspended fibrous membranes with thickness of 10 μm or below are especially technically-demanding. In particular, membranes requiring the combination of low Young's modulus and small thickness will ultimately prohibit the membrane transfer process. Due to the above reasons, conventionally produced fibrous micro-membranes are usually based on fibres of thermoplastic polymers, of which tensile moduli are in the Giga Pascale range [11,12], much higher than those of soft tissues (with bulk tissue stiffness typically below 100 MPa).

Addressing the above challenges, we present technical advancements in fabricating ECM-laden fibres and suspended fibrous membranes that can be directly patterned on target substrates. To our knowledge, this is one of the first techniques which enable *in situ* biologic micromembrane fabrication. Our method, utilising a low-voltage electrospinning (LEP) mechanism, results in up to 50 wt% content of ECM in the fibre dry weight. The use of gelatin as a carrier polymer to encapsulate the ECM leads to mechanically soft fibres, demonstrating single-fibre tensile moduli between 200 kPa and 20 MPa depending on the ECM content. The combination of solvents and cross-linker used enable the retention of some key ECM biologic components post-fabrication, and are also expected to impose lower cytotoxicity than some previous systems (see discussion below). The ECM-laden fibre patterning method presented here will see potential applications in *in vitro* assays, and tailoring structure and biological functions of tissue engineering scaffolds.

2. Materials and methods

2.1. Matrix decellularisation

Urinary bladder matrix (UBM) was prepared as previously described [13]. Porcine urinary bladders from market-weight animals were acquired from Tissue Source, LLC. Briefly, the tunica serosa, tunica muscularis externa, tunica submucosa, and tunica muscularis mucosa were mechanically removed. The luminal urothelial cells of the tunica mucosa were dissociated from the basement membrane by washing with deionized water. The remaining tissue consisted of basement membrane and subjacent lamina propria was decellularised by agitation in 0.1% peracetic acid with 4% ethanol for 2 h at 300 rpm. The tissue was then extensively rinsed with PBS and sterile water. The UBM was then lyophilized and milled into particulate form using a Wiley Mill (Thomas Scientific, NJ) with a #60 mesh screen [14].

2.2. Materials and solution preparation

Urinary bladder matrix (UBM) was used as a model ECM due to its established extraction protocol, accessibility, and characterised biochemical compositions [3,15–17], as above. Gelatin (from porcine skin) powder was obtained from Sigma-Aldrich G1890 (Lot SLBC8470V). Solvents of glacial acetic acid and ethyl acetate were obtained from Merck Millipore 100,063 and 100789, respectively. Glyoxal was obtained from Sigma-Aldrich 128465.

For generating fibres, solutions of ECM were prepared in order to feed to the low-voltage electrospinning process. Dehydrated gelatin and UBM powder were dissolved in an aqueous solution combining deionised water, acetic acid and ethyl acetate according to the weight percentages shown in Table 1 below. The solution was stirred at room temperatures until homogenised (which can be identified by the homogeneity of the solution color). To obtain insoluble fibres, 3 wt% glyoxal was added to the solution as a cross-linker immediately prior to the electrospinning process.

2.3. Low-voltage continuous electrospinning patterning (LEP)

A modified LEP process from [18,19] is utilised to create fibre patterns. A desired ECM-laden solution was dispensed using a 1 mL syringe and pumped at a rate ranging from 1 to 5 μL/min. A DC voltage of typically 230 V was applied between the syringe tip and a moving stage that held substrates to collect the as-spun fibres. Electrospinning was initialised using glass slides placed at the two ends of the deposition paths. By programming the

Table 1
Composition of electrospinning solutions.

ECM-laden solution	UBM (wt%)	Gelatin (wt%)	Water (wt%)	Acetic acid (wt%)	Ethyl acetate (wt%)	Final concentration of ECM in fibre (wt%)
0 wt% ECM	0	19.0	26	33	22	0
1 wt% ECM	0.19	18.8	26	33	22	1
10 wt% ECM	1.9	18.1	26	33	22	10
50 wt% ECM	9.5	9.5	26	33	22	50

movement of the stage using Labview, the polymer jet could be regularly patterned onto the substrates. A typical writing process includes the stage acceleration set to 1500 mm/s^2, and stage speed at 150 mm/s. The applied voltage was 230 V. The ECM-laden fibres were allowed to crosslink at room conditions for 24 h post LEP. Modifying the LEP process also allows suspended membrane formation on a pre-fabricated device structure, such as over a microfabricated fluidic channel or a 3D printed construct. In this case, the device structure was placed on the moving stage in between the initiators. Fig. 1b demonstrates the setup of a low voltage electrospinning system.

2.4. Morphological characterisation of single fibres and membrane constructs

For scanning electron microscopy (SEM) imaging, samples were coated with Platinum for 60 s, and subsequently imaged by a FEI Nova NanoSEM.

For confocal microscope imaging of the 3D profile of the membrane structure, 1 wt% sodium fluorescein (F2456 Aldrich) was added to the polymer solution prior to LEP. The samples were imaged using a Leica TCS SP5 microscope. To reconstruct the 3D configuration, a z-stack was acquired over a 100 μm thickness with a 0.5 μm interval. The z-stack was converted into 3D image profiles using ImageJ.

AFM maps were realized by means of a JPK nanowizard2 (Germany) system operating in tapping mode and equipped with a silicon tip (μmasch, 2 Nm^{-1}) with a nominal radius of 10 nm. Image flattening and roughness analysis was performed by SPIP (Image metrology, Denmark) software.

2.5. Chemical and biochemical characterisation of as-spun fibres

Immunofluorescent staining was performed to characterise the presence of fibronectin and collagen IV in 0 wt% ECM fibres and 50 wt% ECM fibres. In the first group (Fig. 2b), both the vertical and horizontal fibres were 0 wt% fibres, whereas in the second group (Fig. 2c), 50 wt% ECM fibres were spun vertically, and 0 wt% ECM fibres spun horizontally. The antibodies used are anti-transglutaminase 2 (mouse monoclonal, Abcam ab2386), anti-collagen IV (rabbit polyclonal, Abcam ab6586), and anti-fibronectin (ab23751, Rabbit polyclonal to Fibronectin). Once the ECM-laden fibres were patterned onto a glass coverslip and fully crosslinked, the samples were blocked with 3% BSA/PBS for 1 h. After washing the sample with PBS (ThermoFisher 10010023), primary antibodies were added and the samples were incubated for 1 h. Subsequently, the samples were washed again with PBS and incubated with secondary antibodies for 1 h. After a final wash, the samples were stored in mineral oil and imaged within two days.

Energy-dispersive X-ray spectroscopy (EDX) elemental analysis was performed on the fibres using a FEI Nova NanoSEM. Suspended fibres patterned over a 3D-printed holder was used for this purpose. As the fibres were suspended and not attached to any backing substrate, potential background contamination was eliminated. The fibres were coated with Platinum for 45 s. An acceleration voltage of 10 kV was used in the EDX measurement. Once the fibre was imaged in focus, 5 points were taken along the fibre centre. At least 10 fibres were measured for each fibre composition, to obtain statistical data. The elements were identified, and their concentrations were measured using the manufacturer's in-built program.

Fourier transform infrared spectroscopy (FT-IR, Bruker IFS 113v) was used to measure the molecular structures in the raw ECM powder, protein references and ECM-laden fibres. References formed by collagen I and IV, gelatin and ECM-laden solutions were deposited on a glass petri-dish and dried for 24 h. Dry films were obtained and measured. The ECM-laden fibres were patterned onto silicon wafers using LEP. The fibres were removed using a razor blade and collected for measurement. Attenuated total reflection infrared spectroscopy (ATR-FTIR) was performed using a Bruker Vertex 70 spectrometer equipped with a diamond ATR element. Spectra were acquired with a resolution of 4 cm^{-1} and they were processed by means of Origin Pro software. They were first averaged (3 spectra with 128 co-averages) and then normalized to their maximum. Second derivatives of the spectra were calculated to deconvolve structural contributions within the amide band I.

2.6. Single fibre mechanical characterisation in situ

A micropipette cantilever method similar to [20] was used to determine the tensile mechanical property of single fibres. Calibrated micropipette cantilevers (with an outer diameter of 7.5–10 μm, bending stiffness of 4.20 ± 0.05 mN/m to 9.13 ± 0.17 mN/m) were fixed onto the arm of an MM3A LMP micromanipulator (Kleindiek Nanotechnik). This was fixed onto the stage of a Zeiss AxioObserver Z1 microscope. A speed of c01 was selected for all axes in the micromanipulator with a frequency of 2.7 Hz. To check the reliability of the cantilever, calibration was performed to each cantilever before and after performing a single fibre measurement. This was to ensure that the measurement process did not cause plastic deformation of the cantilever and the force constant remained valid during the fibre deformation measurement. Dried fibre samples were immersed in water for 1 h for re-hydration. Afterwards a sample was mounted onto the microscope. The suspended fibre was immersed in water in a petri-dish and the measurement was performed in water. Initially, the cantilever was positioned away from the fibre. The micromanipulator was moved through several steps. The distance the cantilever tip travelled in the microscope view was recorded to calculate the cantilever end displacement corresponding to a single step change in the micromanipulator. Afterwards, the cantilever was made to come into contact with the fibre. As the cantilever deformed the fibre, each position of the micromanipulator was recorded. At the same time, snapshots of the fibre deformation were taken. The cantilever deflection was calculated by subtracting the tip displacement deforming the fibre from that due to the micromanipulator movement. The fibre deformation was measured in ImageJ.

2.7. Bulk film mechanical measurement

Bulk films of ECM-laden hydrogels are made into strips with a target width of 10 mm, length of 20 mm and thickness of 1 mm. The film dimensions fluctuated slightly between different preparation runs and were taken into account when calculating the Young's modulus. The films were left to dry and crosslink for 24 h at room temperature. The fully crosslinked films were immersed in distilled water to rehydrate for at least 1 h before measurement. The hydrated films or gels were installed on Instron 5544 and underwent uniaxial deformation at a deformation rate of 0.6 mm/min.

2.8. Cell culture

For the endothelial cell line (EA.hy926) culture, a protocol was adapted from [21] (for a 2D culture) to enable cell culturing on suspending a ECM-laden membrane device. Briefly, the as-fabricated device was first immersed in PBS (ThermoFisher 10010023) for 18 h and in DMEM culture medium for 1 h before cell seeding. Cell seeding was performed at in 500 μL DMEM culture medium at a seeding density of $\sim 1 \times 10^5$ cells per device. Subsequent cell culture was performed at 37 °C and 5% CO2. Cultures were maintained for different time periods depending on the experiment purpose.

For the glomerular cell culture, conditionally immortalised human glomerular endothelial cell (GEnC) lines and podocytes cell lines were obtained and cultured according to [22,23]. A 3D ring-membrane device was immersed in DMEM for 1 h before cell seeding, with the fibrous membrane facing the bottom of the 6-well plate. GEnCs were cultured in a T75 flask at 33°C to reach confluence. After detaching cells using standard trypsin protocol, ~150,000 cells were seeded onto each membrane device. GEnCs were cultured at 37 °C for 24 h before forming a co-culture with podocytes. Podocytes were resuspended in the same manner as GEnCs. After resuspension, the devices were flipped using a pair of sterilised tweezers. 150,000 podocyte cells were seeded on top of the membrane. The single culture and co-culture were maintained at 37 °C for up to 7 days, with culture medium changed every two days.

2.9. Cell viability studies

Cell viability was evaluated used an AlamarBlue® assay. Cells (EA.hy926 or podocytes) were seeded onto glass substrates patterned with pure gelatin or 10 wt% ECM fibres. After a specified incubation time (1, 4, 7, or 11 days), the culture medium was removed and replaced with 10% v/v AlamarBlue reagent. After an incubation of 6 h, the absorption of the supernatant was measured (at wavelengths 570 nm and 600 nm). Culture medium without cells containing 10% v/v AlamarBlue was used as a negative control. Percentage reduction of AlamarBlue was calculated using the manufacturer's formula:

$$\text{Percentage reduction of AlamarBlue} = \frac{(02 \times A1) - (01 \times A2)}{(R1 \times N2) - (R2 \times N1)} \times 100$$

where O1 = molar extinction coefficient (E) of oxidised alamarBlue at 570 nm, O2 = E of oxidised alamarBlue at 600 nm, R1 = E of reduced alamarBlue at 570 nm, R2 = E of reduced alamarBlue at 600 nm, A1 = absorbance of test wells at 570 nm, A2 = absorbance of test wells at 600 nm, N1 = absorbance of negative control well at 570 nm, N2 = absorbance of negative control well at 600 nm. Four biological replicates were used for each condition.

2.10. Fibre remodelling evaluation

The potential fibre degradation effects and fibre remodelling ability were evaluated by three tests. In the first test, cells were cultured on fibres directly adhered on glass substrates. Thus, the fibre pattern configuration is mostly fixed, and the proliferation and alignment of cells following fixed fibre patterns were monitored. In the second test, cells were cultured on sparsely patterned fibres suspended over a channel, of which configuration resembles the micropipette single fibre deformation test stated above. Thus, individual fibres are free to be deformed by cells attached to the fibres, and the cell alignment and fibre configuration were monitored. In the third test, fibres were patterned into a membrane form (with a mesh size smaller than 5 μm) suspended across a channel, the formation of cell sheet on the membrane is monitored. For all the three tests, observations were done under an optical microscope over a 6–7 day period, where images were captured at selected time points at similar regions to monitor the changes.

2.11. Immunofluorescent staining and imaging of fixed samples

For cell fixation, the medium was replaced using absolute ethanol and incubated at −4 °C for 4 h. After washing 3 times with PBS, the sample was immersed in 3% BSA/PBS solution and stored at room temperature for 1 h. Afterwards, the sample was washed with TBS-T 3 times. Primary antibody (1/100 for fibronectin and 1/200 for VE-cadherin and podocin) was added to the sample and stored at room temperature for 1 h. Then, the sample was washed with TBS-T again and the secondary antibody was added and incubated for 1 h at room temperature. The sample was washed with TBS-T and hoescht 33342, and left for 30 min. Finally, the sample was washed with TBS-T and the sample was preserved in mineral oil. A confocal microscope Leica TS5 was used for fluorescence imaging. The argon laser power was at 30% and a 633 NeHe laser was used. The visible laser power was between 10% and 25%, with digital gain between 800 and 1000. The same laser power and gain were used for cross comparison of the samples. The images were captured at 10 Hz.

2.12. Cell fixation for SEM imaging

The cell fixation and SEM imaging protocol were adopted from [24]. The cells were fixed with glutaldehyde and cacodylate buffer solution for 10–15 min. The sample was transferred into pure cacodylate solution for 1 h. Afterwards, the sample was immersed in a 0.1 M osmium/cacodylate/water solution for 15 min. Then the sample was washed in distilled water and immersed in a sequence of ethanol solutions with concentrations of 25%, 50%, 60%, 70%, 80% 90%, and 96% for 10 min each. The sample was then immersed in absolute ethanol for 30 min, with a change of ethanol every 10 min. The sample was loaded in the critical point dryer for 2 h and underwent gold coating. SEM imaging (FEI Nova NanoSEM) was performed one day after the cell preparation.

2.13. Statistical methods

Quantitative data are presented as mean ± standard deviation, and have been statistically analysed using the OriginPro 2017. SEM and AFM images were chosen typical of three imaging samples. The standard deviation of mean square roughness was a measure of three randomly selected areas on the fibres measured. Fibre diameter histogram was an average of over 50 fibres in randomly selected field of views.

EDX was measured for ten fibres for each solution condition. Three points were measured along each fibre. The fluorescence intensities of proteins were measured using ImageJ. For each condition, 3–4 randomly selected horizonal lines and vertical lines were drawn across the fibres, and intensity along each line was measured, see examples in Fig. 2b–c. The peak intensity represents the fluorescence intensity of the fibre. The intensities of fibres obtained were averaged, and the average intensity of vertical fibres was then normalised to the average intensity of horizontal fibres (i.e. vertical intensity dividing horizontal intensity) for each condition. One-way ANOVA was performed to evaluate whether there is any statistical significant difference between the fluorescence intensities in 50 wt% ECM fibres and 0 wt% ECM fibres.

3. Results and discussions

3.1. Material selection rationale

To impart solution process-ability and electrospinnability, various solvents have been studied for dissolving large protein molecules [25–27]. Although solvents such as hexafluoro-2-propanol (HFP) are commonly used for dissolving collagen I and gelatin materials to produce an electrospinnable solution [26], HFP leads to significantly degraded secondary and tertiary protein structures, which are undesirable [28,29]. In our method, water-based solvents with a mixture of acetic acid and ethyl acetate were chosen, where both reagents are known to have lower toxicity than

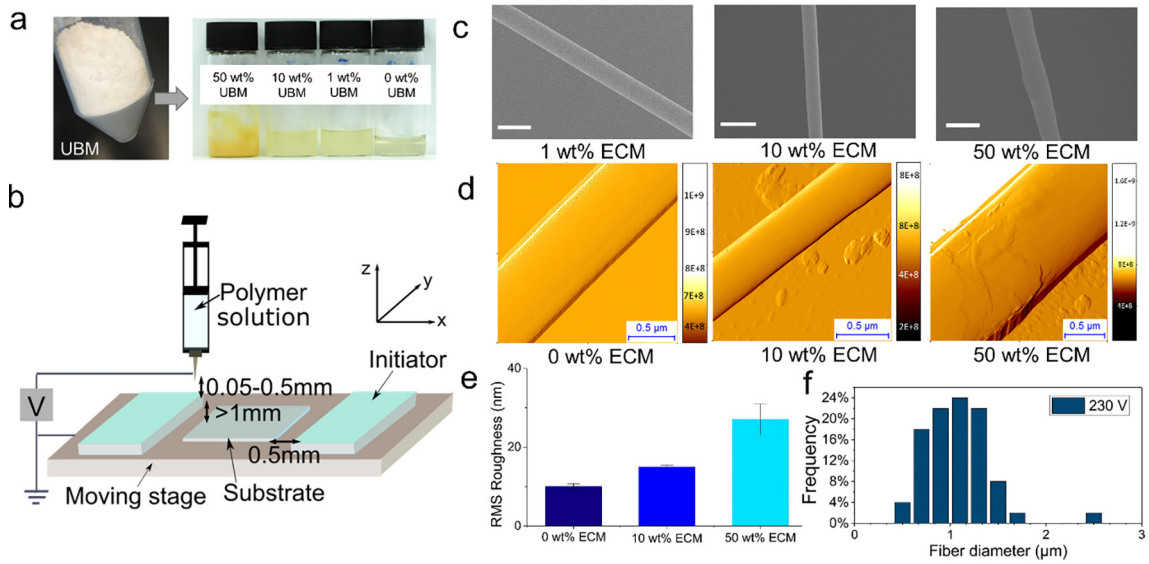

Fig. 1. (a) Four electrospinning solutions with 0 wt%, 1 wt%, 10 wt% and 50 wt% of UBM were prepared by mixing the UBM powder with gelatin, water, acetic acid and ethyl acetate; (b) Schematic diagram of the low-voltage electrospinning setup; (c) SEM micrographs of fibre surface morphology. Scale bars 1 μm; (d) AFM morphology maps of fibre surface morphology; (e) Mean squared roughness of fibres with different ECM compositions; (f) Distribution of fibre diameters when fibres were fabricated at 230 V (n = 50).

HFP (LD50 for rats is 3310 mg/kg for acetic acid [30] and 5620 mg/kg for ethyl acetate [31], in comparison to 1500 mg/kg for HFP [32]). The solvent choice is also of paramount importance in preserving the chemical structures of the dissolved molecules. Acetic acid is widely used as a denaturant in solubilizing growth factors [33], ECM proteins [34] and nucleic acid [35]. Although this can potentially affect protein folding and bioactivities, it is a necessary solvent to solubilize high concentrations of gelatin for electrospinning. Our results below will demonstrate that the acid has only limited effects on the ECM protein denaturing. Finally, ethyl acetate was used to lower the surface tension of the combined solution.

For the crosslinker choice, among various methods of crosslinking gelatin and solubilised collagen, glyoxal was chosen in our study. Other common protein crosslinkers include carbodiimide (EDC) for carboxyl groups, NHS ester and glutaraldehyde for amine groups, maleimide for sulfhydryl groups, and hydrazide for carbonyl groups [36]. Glyoxal is a homobifunctional crosslinker [37]. The toxicity level of glyoxal is lower than that of formaldehyde and glutaraldehyde (LD50 for rat is 640–8979 mg/kg for glyoxal [38], in comparison to 600–800 mg/kg for formaldehyde [39] and 246 mg/kg for glutaraldehyde [40]). Glyoxal has been proven to successfully crosslink gelatin [41]. To prove the functional properties of the crosslinked fibres, biochemical analysis, *in situ* mechanical test and cell culture studies were performed, of which results are to be illustrated below.

3.2. High content ECM-laden fibres from LEP

Based on the solution preparation and the initiator-based LEP process [18], we were able to obtain up to 50 wt% of ECM in a gelatin fibre matrix, much higher than a previous report performed by far-field electrospinning using the same matrix [10]. We attribute this ability to incorporate high concentrations of ECM 'fillers' to the LEP configuration, which uses initiators to break up the pendant droplet for fibre drawing (see detailed mechanism in [18]). Without initiators, pure gelatin fibres can be processed using a near-field electrospinning (NFES) method at a higher applied voltage [21]. However, as ECM content was added beyond 10 wt%, no fibres can be produced with NFES even at high voltages (>1000 V). Thus, an initiator-based mechanism in LEP is critical to enable high loadings of ECM proteins in fibres.

Typical microscopic morphologies of single fibres were shown in Fig. 1c–d. SEM shows that fibre surfaces appeared to be homogeneous and smooth, for all the ECM contents investigated in this work. However, AFM mapping shows a more intricate structure with the presence of a fibre-like surface topography, which is dependent on the ECM content. For 50 wt% ECM content, the fibre surface has a rough appearance. Plotting the root mean square (RMS) roughness in Fig. 1e showed that surface roughness increased with ECM concentration in fibres. This result strongly implies that the ECMs were present as partially dissolved clusters encapsulated in the fibre matrix.

3.3. Fibre chemical and biochemical constituents

Elemental compositions of the ECM-laden fibres were determined by EDX, shown in Fig. 2a. ECM is known to consist mainly of organic compounds containing four elements: hydrogen H, carbon C, oxygen O and nitrogen N. Traces of sulphur S can also be found. The sensitivity of the concentration detection is normally 0.1 wt% and the spatial resolution is 1 μm; EDX cannot be applied for detecting hydrogen. Fig. 2a shows that the degree of composition variation among the fibres was the lowest in 0 wt% ECM fibre. As ECM was incorporated, all the statistical variations in C, N and O increased even for 1 wt% addition. This result suggests that the ECM content was not fully dissolved in the gelatin matrix. The variation of protein groups between the ECM rich region and the gelatin rich region can bring variations in the chemical element proportions at the area of measurement along a fibre. Although there are ECM rich and gelatin rich phases within the fibre, we suggest that the distribution of these two phases are reasonably even throughout. This is supported by the consistency in the mechanical measurement results for single fibres versus bulk films; and further the even distribution of mono-culture cells on membranes to be illustrated below.

Collagen IV and fibronectin, as the representative proteins in ECM, are known to be present in urinary bladder matrices (UBM) [15]. The presence of these proteins was characterised using

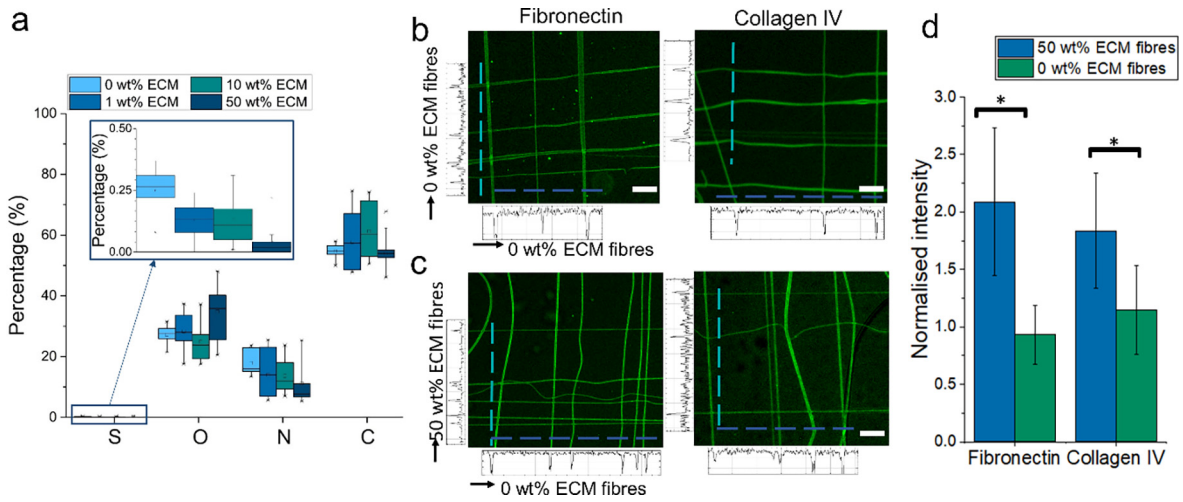

Fig. 2. (a) Compositions of sulphur, oxygen, nitrogen and carbon elements in ECM-laden fibres characterised by EDX; (b–c) Confocal microscopic images show the fibronectin and collagen IV stainings in (b) 0 wt% ECM fibres (both vertical and horizontal fibres) and (c) in 50 wt% ECM fibres (vertical fibres) and 0 wt% ECM fibres (horizontal fibres). Scale bars 50 μm; for each condition, intensity was measured along 3–4 horizontal and vertical lines (example intensity spectrum was shown next to the dashed line). The peak value of the spectrum represents the fluorescence intensity from the fibres. In total, 97–66 fibre sections were measured for each condition. (d) Average fluorescence intensity of fibronectin and collagen IV staining in vertical fibres normalised to the average intensity of horizontal fibres. Statistical significance was evaluated using one-way ANOVA. $p^* < 0.05$.

immunofluorescent staining methods. Measurements were performed on two groups. The first group contained 0 wt% ECM fibres only (Fig. 2a, b) and the second group contained 0 wt% ECM fibres in the horizontal direction and 50 wt% ECM fibres in the orthogonal direction (Fig. 2a, c). Negative controls were performed for each protein, by omitting the primary antibody and only using the secondary antibody.

As shown in Fig. 2d, the normalised intensities of fibronectin and collagen IV in the first group (0 wt% ECM fibres) were approximately equal to 1. This indicates no significant difference between the fluorescence intensity of the horizontal and the vertical fibres in the first group, which is as expected for the pure gelatin composition. In comparison, the normalised intensities for both the fibronectin and collagen IV staining in the 50 wt% ECM fibres were significantly above 1. This suggests that the additional fluorescence signals are arising from the selected ECM presence in the fibres. Thus, the fibre processing method has retained the bioactivities of the ECM components.

In addition to the above analytical techniques, FTIR was also used to evaluate whether the solution preparation method and the LEP process have affected the protein structural folding. First, we confirmed that the ECM powder contains proteins in their pristine conformations by comparing the spectra of the normalised sum of the reference proteins (collagen I, collagen IV and gelatin) with the ECM powder (Fig. S1). In particular, amide I band is of interest due to its sensitivity to the secondary and quaternary protein structural conformations [42]. Fig. S1c and e show that the ECM powder spectrum and the spectrum of the normalised sum of reference proteins possess similar amide I band position and shape, confirming a highly similar structural conformation. The ECM power shows, respect to the protein spectrum, additional peaks at 1740 cm^{-1} (C═O stretching), 2920 cm^{-1} and 2870 cm^{-1} (asymmetric and symmetric CH_2 stretching). These peaks are associated with the lipid residual presence in the ECM powder (Fig. S1c–f) [42].

To evaluate the influence of the solution preparation method on the protein conformations, we compared the spectra of ECM-laden gelatin films with the ECM powder (Fig. 3a–c). The second derivative analysis at amide I band in Fig. 3C, which allows to deconvolve the structural contributions in the amide I band, shows that all the films share similar peak shape and positions. This high similarity indicates a high similarity in secondary and quaternary structure of protein conformation within the samples (Fig. 3c). Using the lipid peaks (i.e. C═O stretching 1740 cm^{-1}, and CH_2 stretching 2920 cm^{-1} and 2870 cm^{-1}) as indicators, we observed that the lipid content increased as a function of the ECM content in gelatin. This highlights the successful incorporation of the ECM into the films, without a perturbation of the native conformation of proteins in the matrix.

Finally, we compared the spectrum of 10% ECM fibre with the 10% casted film to determine if the LEP process imposed any significant chemical degradation to the proteins (Fig. 3d–f). Detailed analyses in Fig. 3e–f show that nearly identical shapes of the FTIR spectra and their second derivatives. Hence, we conclude that, firstly, the solution preparation method did not impose measurable effects on the secondary and quaternary structures of the ECM proteins; and secondly, no measurable chemical degradation occurred to the proteins and no reduction in ECM protein content is induced using LEP to process the solution.

3.4. Mechanical properties of single fibres

Cells are known to be sensitive to the mechanical properties of substrates [43,44]. In the present study, the Young's moduli of individual ECM-laden fibres were measured using a glass capillary cantilever method. Fig. 4a shows a typical set of snapshots when a fibre was under deformation. Fig. 4b shows stress versus strain curves for different fibre compositions. This indicates the elastic nature of the sample fibres within the deformation range, thus the gradient of the fitted line corresponds to the Young's modulus (E) of the fibres. Table 2 summarises the Young's modulus values, indicating a clear trend of increased Young's modulus due to the incorporation of ECM component. Compared to the reference films (tensile stress versus strain curves can be found in Fig. S2), the fibres have similar Young's moduli to the bulk film sample at the same ECM concentration. Within the measurement range, the stress was linearly related to the strain for all samples.

The material stiffening effect because of decellularisation was well known. For example, study performed by Beachley et al. [45] reports that the elastic moduli of dried ECM spots (i.e. in a

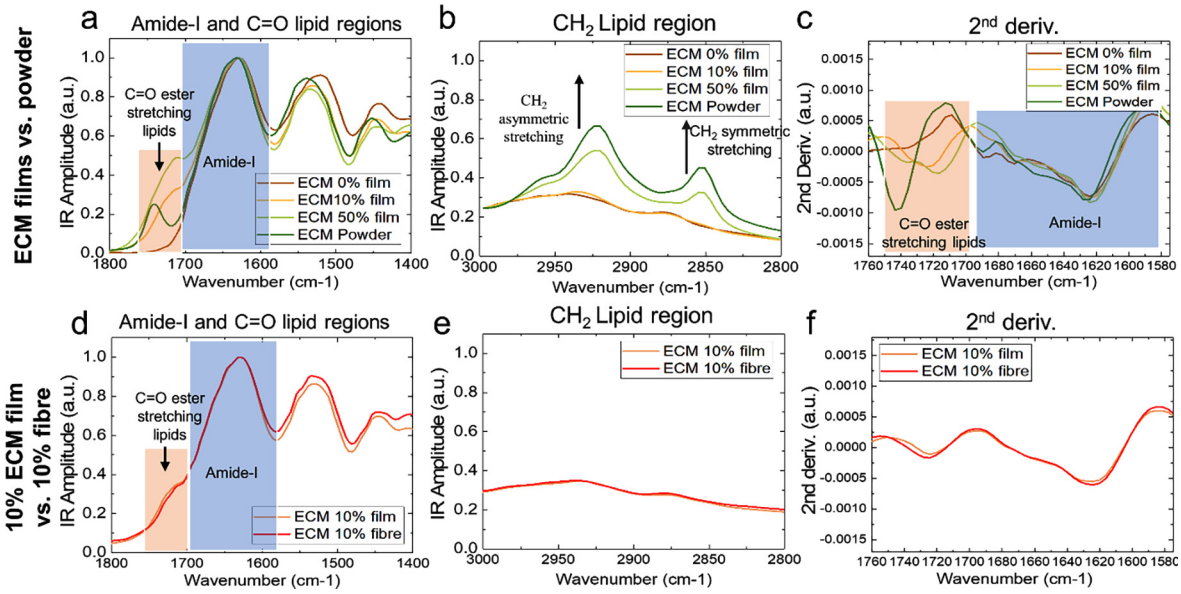

Fig. 3. FTIR spectra comparing (a–c) ECM-gelatin films with different ECM contents with the ECM powder and (d–f) the 10% ECM film with the 10% ECM fibre. Peaks at 1580–1700 cm^{-1} represent the amide-I band which is sensitive to the conformation change in the secondary and quaternary protein structures. Peaks at 1740 cm^{-1} (C═O stretching), 2870 cm^{-1} and 2920 cm^{-1} (symmetric and asymmetric CH2 stretching) are associated with the content of lipids in the samples.

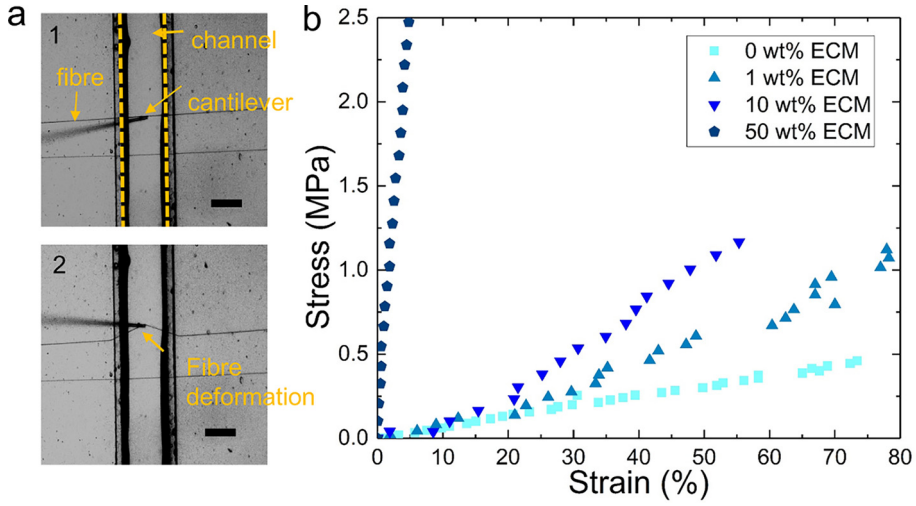

Fig. 4. (a) Micropipette cantilever method to determine the tensile modulus of a single fibre. Fibre was deformed by a cantilever. The deflection of cantilever was measured for calculating stress and fibre deformation. Scale bars 100 μm; (b) Stress–strain curves of fibres with different ECM compositions.

Table 2
Young's moduli and failure strain of fibres and films with different ECM compositions. The value of Young's modulus increased with the composition of ECM. Fibres and reference films at the same ECM composition have similar values of Young's modulus.

	0 wt% ECM	1 wt% ECM	10 wt% ECM	50 wt% ECM
E (fibre) (MPa)	0.61 ± 0.01	1.25 ± 0.17	2.25 ± 0.10	49.0 ± 0.7
Failure strain (fibre) (%)	73.4 ± 3.5	63.7 ± 4.4	55.3 ± 3.4	>6.2
E (film) (MPa)	0.59 ± 0.02	1.57 ± 0.15	3.19 ± 0.16	N/A
Failure strain (film) (%)	120.0 ± 2.5	83.3 ± 1.3	26.7 ± 1.4	N/A

powder form similar to our homogenised UBM) were at least two orders of magnitude higher than that of fresh, hydrated tissues. Although there is large variation in inherent stiffness between native, hydrated tissues, the difference is much less in dried ECMs. In fact, Beachley et al's results show that the stiffness of the ECM spots was all in the GPa range for a range of tissues including brain. Thus, for our results here, the stiffening of fibres for higher ECM concentration can be explained by the physical entanglement of gelatin matrix with the stiff, sub-micron sized ECM clusters. If one considers the additional ECM as suspension particles (as previously also suggested in the AFM and biochemical data), and neglects the charge and molecular interaction, the increase in the volume fraction (concentration) of the ECM will provide an increase in Young's modulus. This reinforcement effect due to

ECM cluster is suggested to be similar to the nanoparticle reinforcement of fibre matrices [46].

Bulk mechanical measurements in prior studies reported Young's moduli of as-harvested bladder to be between 0.03 and 0.20 MPa [47,48], and this was increased to 0.65 MPa for a hydrated decellularised bladder matrix [48]. It is important to note that our study here has reported the Young's modulus measured at the single fibre (building block) level, tuneable between 0.6 and 49 MPa. The single fibre tensile Young's modulus will give an upper limit for the global Young's modulus of a scaffold or a membrane constructed by the fibre building blocks. This is because the mechanical properties of a scaffold/membrane measured at bulk will enviably dependent on the constituent fibre spatial arrangements [49], of which bulk Young's modulus will always be equal to or lower than the single fibre Young's modulus, since the inter-fibre space in a scaffold is filled by cells/ liquid/ air. Thus, we suggest that the ECM-laden fibres produced by our techniques give reasonable approximation to the tissue properties; in particular, they are much 'softer' than the fibrous structures produced by electrospun thermoplastic materials (see Introduction). The fibre remodelling potential by cultured cells is further discussed in a later section.

3.5. Influence of fibres on cellular activity

To evaluate the effects of the fibre compositions on cellular activity, an alamarBlue assay was performed. Reduction of the dye following a defined culture period indicates cellular activity. Cells were cultured on glass slides (as a control) or pure gelatin fibres on glass slides. EA.hy926 cells remained highly active regardless of substrate, as indicated in Fig. S3a with percentage reduction remaining above 70% for both substrates at all time points. Podocytes were cultured on glass slides (as a control), pure gelatin fibres or 10 wt% ECM fibres on glass slides. Since the podocytes were maintained at a non-permissive temperature at which they are intended to be non-proliferative, Fig. S3b shows that the podocyte cellular activity was overall lower than that of the EA. hy926 cells for all conditions. At days 4, 7, and 11, a noticeable increase in cellular activity was observed in cells cultured on the fibre constructs compared to the control. This suggests that for the podocyte culture, the fibre construct supports a slightly higher cellular viability than glass, and hinting the possible importance of the attachment factors or surface topography presented by gelatin or ECM fibres in comparison to bare glass substrates. Overall, results from the alamarBlue assay suggests that cellular activity is unaffected or even slightly enhanced by interfacing pure gelatin or 10 wt% ECM fibres with the cell types investigated here.

3.6. ECM-laden fibres and membranes for cell culture

Programming the x-y stage path allows us to suspend fibres over a gap with robust attachment on the edge of the gap. With more fibre deposition, one can subsequently form a suspended membrane on a device structure, see examples in Fig. 5a–c. A unique advantage of this *in situ* membrane formation process is the devoid of delicate fibre or membrane transfer, attachment and adhesion process [49,50]. Thus, fibres or thin membrane structures, with tuneable mesh size of varying connecting fibre number, can be deposited and attached directly over a channel structure. In Fig. 5e, different mesh sizes were shown to influence the endothelial cell (EA.hy926) lining morphologies within 24 h for pure gelatin suspended membranes.

Since fibre and membrane structures are widely used in *in vitro* cell culture experiments, we then investigate the potential of culturing cells on ECM-laden fibre constructs. An ECM concentration of 10 wt% in gelatin (dry weight) was chosen for

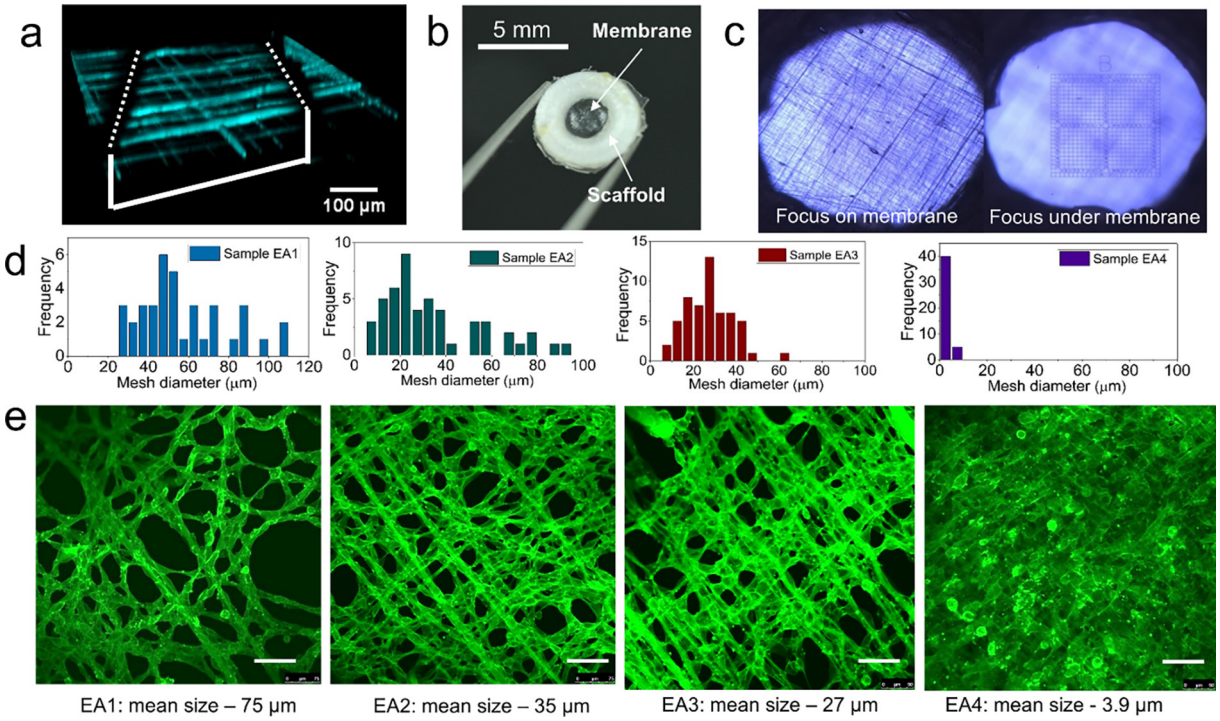

Fig. 5. (a) A suspended fibre network membrane fabricated by LEP under a voltage of 230 V; (b) A suspended membrane patterned on a 3D printed ring device; (c) Images of a thin membrane under microscope; (d) Mesh size distribution of each sample. Samples EA1, EA2, EA3 and EA 4 have a mean mesh size of 75, 35, 27 and 3.9 μm respectively; (e) Confocal micrographs showing EAhy926 morphology difference cultured on pure gelatin membranes with different mesh sizes. Cultures were fixed 24 h after seeding, where F-actin staining (green) is shown. Scale bars 75 μm. (For interpretation of the references to colour in this figure legend, the reader is referred to the web version of this article.)

testing the cell-fibre interaction. Since the ECM particles used here were dehydrated, concentrated forms of ECM, we expect the 10 wt% ECM concentration will give a balanced biochemical attribute versus biochemical attribute in replicating a soft membrane matrix environment. In the results below, we report feasibility cell culture studies based on the endothelial and glomerulus cells, which may provide culture systems warranting more detailed mechanistic studies and functional culture optimisation in the future.

3.6.1. Fibre and membrane mesh remodelling potential

First, the ability of EA.hy926 cells to deform the as-produced fibres were investigated; this was performed by comparing cell cultures maintained on three pure gelatin fibre configurations: fibres attached on glass, fibres suspended sparsely across a channel, and fibres forming a membrane with dense mesh. In the first test, the fibre pattern configuration was mostly fixed on the glass substrate like in our previous work [21]. Fig. S4a shows that at day 1, cells form aligned patterns following those of the fibres,

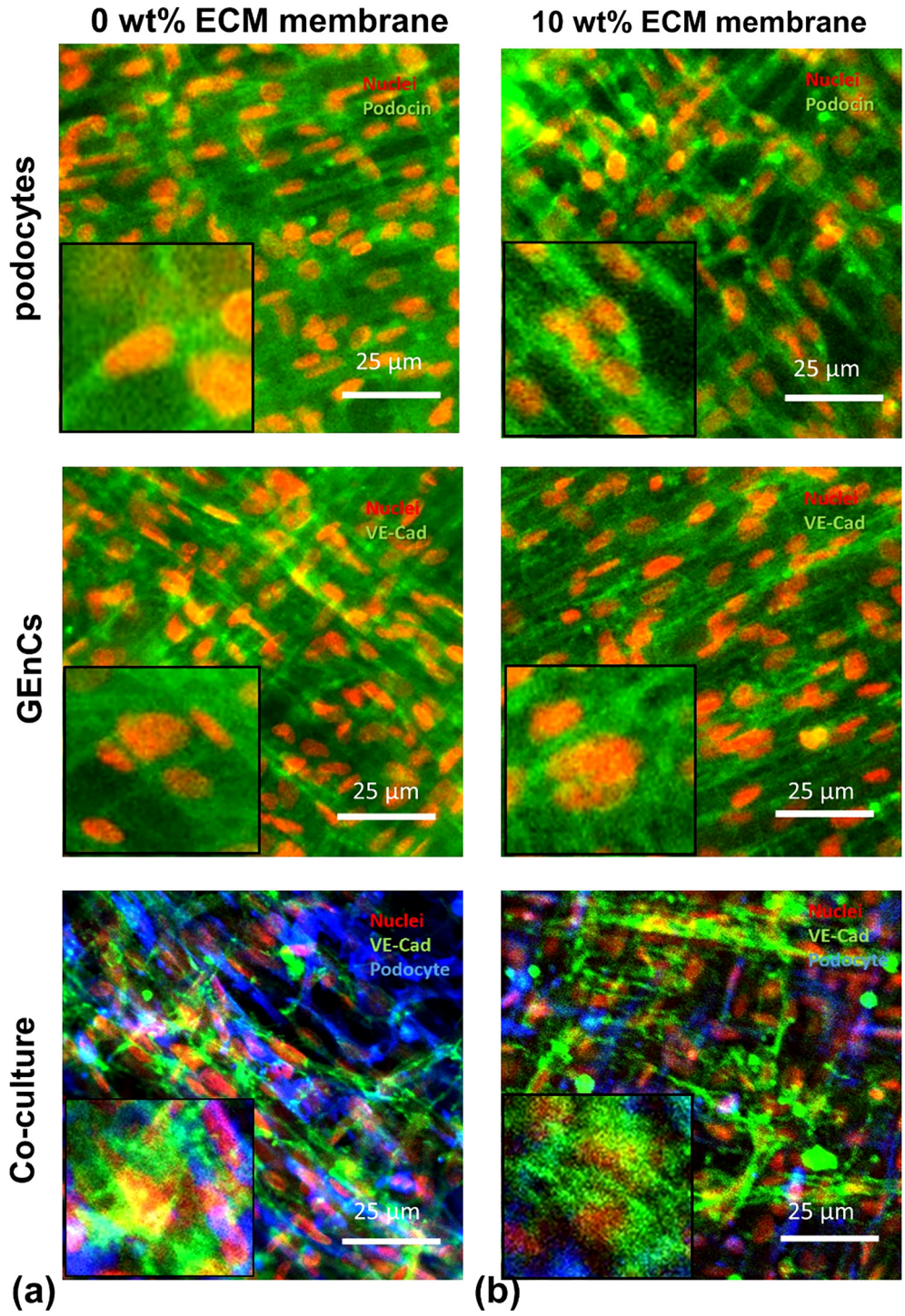

Fig. 6. Immunofluorescence micrographs of GEnCs and podocytes mono-cultures and co-cultures on (a) a 0 wt% ECM membrane and (b) a 10 wt% ECM membrane. Example higher magnification images for the co-culture systems are shown in Fig. S7.

showing distinct orientations differing from the cells attached on the fibre-free space (i.e. glass substrate). As culture time increased, cells proliferated, and it is apparent that the density of cells accumulated on the fibre pattern increased. Despite the increased cell population, the cell patterns remained similar to the pre-formed fibre patterns. In the second test, it is noticeable in Fig. S4b that fibres can be deformed by cells attached and aligned to the fibres; and the sparse fibre network was gradually contracted as the population of cells increased on the fibre over time. In the third test, as shown in Fig. S5a, cell sheet initially formed on the membrane exhibit sparse gaps; however, the size of the gaps increased over the culturing time. Cross-comparing observations from the above three tests suggests that, firstly, fibres fabricated with our method do not display noticeable chemical degradation within 7 days (especially supported by test 1 and 2). Secondly, the fibre pattern configurations control the cells' ability in mechanically remodelling the fibrous matrix, which would warrant more detailed, systematic investigations in the future.

In comparison to pure gelatin membrane (i.e. 0 wt% ECM membrane in Fig. S5a), the use of 10 wt% ECM membranes were shown to reduce the fibre matrix remodelling ability of EA.hy926 cells during the formation of cell sheets. As shown in Fig. S5b, cells culture on the 10 wt% ECM membrane underwent little fibre matrix re-organisation. In fact, some initial 'gaps' were closed due to the increased cell population on the membrane over time. The reduced matrix remodelling effects can be due to different reasons. Firstly, it could be a simple mechanical effect as a result of the increased single fibre stiffness due to the ECM incorporation; other possibilities are the biochemical factors provided by the ECM (such as collagen IV) can provide a more quiescent phenotype of the endothelial cells [51].

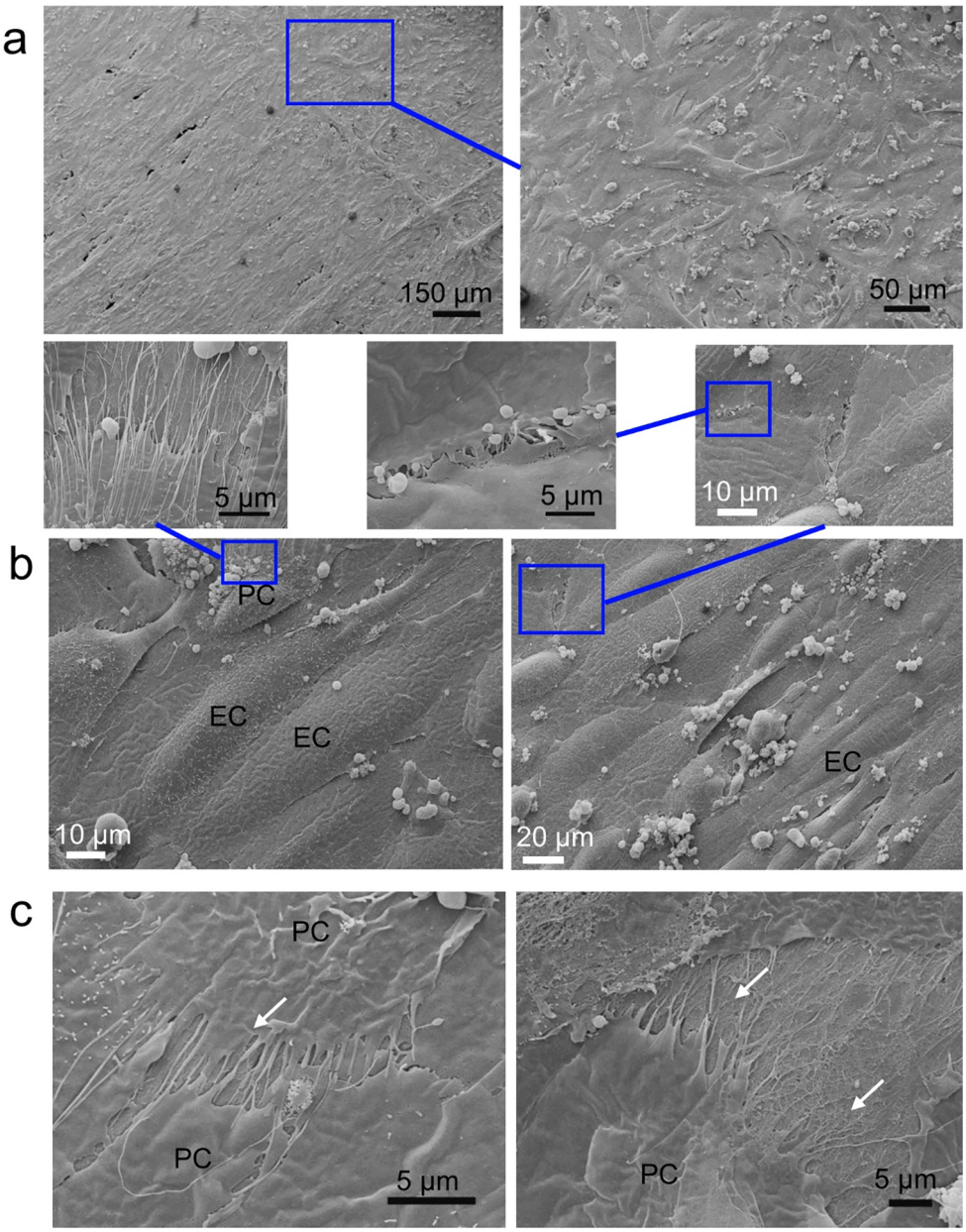

Fig. 7. SEM micrographs showing (a) a cell sheet evenly covering the surface of membrane; (b) Regions displaying cell morphology predominantly akin to those of endothelial cells (EC); (c) Regions displaying cell morphology akin to those of podocytes (PC) with processes indicated by arrows.

3.6.2. Membrane structures for glomerular cell cultures

For the podocytes and GEnCs co-culture, our original aim was to form a tri-layer structure (podocytes – membrane – GEnC), in order to resemble the form of a glomerular filtration membrane. Membranes with a high mesh density (i.e. mesh size smaller than 5 μm) were patterned and suspended on a 3D printed ring in a configuration resembling a trans-well insert configuration, where cells can be seeded on a single side, or both sides of the membrane.

A number of key observations are made. First, it is important to note that cell 'sheets' of podocytes and GEnC can be formed fully covering the native membrane, without additional ECM coatings (see Fig. 6 and Fig. S6). This is in stark contrast to systems utilising thermoplastic fibrous membranes or PDMS membranes, where either podocyte specific and GEnC specific ECM factors should be applied to the membranes to facilitate cell attachment [52]. Secondly, cross-comparing the ECM-laden system with the pure gelatin system, the ECM-laden membrane seems to produce different levels of podocin and VE-Cad expressions in the mono-culture systems, where the addition of ECM seems to increase the corresponding protein expressions, see Fig. S7c. However, we were not able to provide complementary semi-quantitative analysis using techniques such as Western blots at this stage, due to the relatively low cell numbers. Third, although the monoculture of GEnCs were able to form a dense cell sheet on the membrane, the addition of podocytes on the other side of the membrane gave rise to a re-organised cellular distribution between the two cell types. The originally intended tri-layer structure was no longer maintained after 7 days of culture, where aggregation of GEnCs among podocytes was seen (evidenced comparing Fig. 6a–b, and Fig. S6a–b). Further SEM image, Fig. 7a, shows a confluent layer of cell sheet evenly covering the entire membrane surface. Such a cell sheet morphology is different to that created based on electrospun thermoplastic polymer membrane [53]. In particular, the cell sheet formed on the LEP ECM-laden membrane shows preferred cell-cell interconnection (Fig. 7b–c) than the cell-fibre interconnection observed in the thermoplastic fibre case. Due to the fact that a membrane surface would consist of both the GEnCs and podocyte cell types due to cellular re-organisation, our SEM images show morphological phenotypes of both endothelial and podocyte cells. Although a tri-layer structure did not form under our culture conditions, our results reflect the potential importance of ECM incorporation, and the fibre mechanical properties in permitting cellular re-organisation, in a trans-membrane context. Whether the ECM laden in the gelatin fibres would be effective in modifying cellular biological response, requires further detailed quantitative analysis for confirmation.

4. Conclusions

ECM-laden micro-nano-fibres and membranes were fabricated with an ECM content of up to 50 wt% in gelatin. The low voltage application as well as the incorporation of initiators in LEP, have enabled the patterning of suspended fibrous structures *in situ*, directly on complex planar geometries, such as 3D printed holders and microfluidic channels. Results from the fibre chemical analysis support the proposition that multiple ECM protein components have remained active within the fibre and membrane structures post ECM biofabrication. Combining results from AFM, EDX, and single fibre mechanical measurement, it is evident that the ECM remained as partially dissolved clusters, which was encapsulated within the fibre gelatin matrix. We suggest this may be the key reason enabling optimal preservation of the ECM biochemical activity and the ECM protein conformation during acidic solvent processing: limited acid contents have penetrated inside the ECM particulate to unfold the molecular structures. Compared with existing fibrous membrane device systems, the ECM-laden fibre membrane demonstrated here exhibits unique attributes in its low fibre stiffness, small membrane thickness, in addition to the ability to incorporate active ECM components. This cell culture model effectively permitted cell adhesion for EA.hy926 endothelial cells, and human podocyte and glomerular endothelial cell lines, without the application of extra cell specific ECM coatings. The unexpected result in the re-organisation of the podocyte-GEnC seen in the trans-membrane co-culture model will warrant further studies. In particular, it will be interesting to compare to the case of a conventional trans-well membrane system, where cells are forced to assemble into a tri-layer structure interfacing a non-modellable membrane. Looking ahead, the ECM fibre patterning capability demonstrated here can be built on for incorporating soft ECM protein scaffolds into different devices for other biological models. Compared to a whole organ decellularised organ scaffold, it is expected that a biofabricated ECM culture device will provide advantages for simple recellularization, culturing of multiple cell types and quality checks, seeing favourable attributes for *in vitro* culture applications in particular as drug testing platforms.

Acknowledgements

This work is supported by the Engineering and Physical Sciences Research Council (EPSRC) UK (EP/M018989/1) and European Research Council (ERC-StG, 758865). The authors thank the studentship and funding supports from the EPSRC DTA (Z.L.), the WD Armstrong Trust (I.M.L), the Swiss National Science Foundation (P300P2_171219) and the Centre for Misfolding Disease of the University of Cambridge (F.S.R.). We are grateful for the assistances of Mr. Alex Casabuena in SEM imaging, Mrs Lan Ni in cell culture and Mr Simon Griggs in EDX measurement.

Appendix A. Supplementary material

Supplementary data associated with this article can be found, in the online version, at https://doi.org/10.1016/j.actbio.2018.08.010.

References

[1] S.F. Badylak, The extracellular matrix as a scaffold for tissue reconstruction, Semin. Cell Dev. Biol. 13 (2002) 377–383.
[2] R.N. Chen, H.O. Ho, Y.T. Tsai, M.T. Sheu, Process development of an acellular dermal matrix (ADM) for biomedical applications, Biomaterials 25 (2004) 2679–2686.
[3] T.W. Gilbert, D.B. Stolz, F. Biancaniello, A. Simmons-Byrd, S.F. Badylak, Production and characterization of ECM powder: Implications for tissue engineering applications, Biomaterials 26 (2005) 1431–1435.
[4] H.C. Ott, T.S. Matthiesen, S.-K. Goh, L.D. Black, S.M. Kren, T.I. Netoff, D.A. Taylor, Perfusion-decellularized matrix: using nature's platform to engineer a bioartificial heart, Nat. Med. 14 (2008) 213–221.
[5] T.W. Gilbert, T.L. Sellaro, S.F. Badylak, Decellularization of tissues and organs, Biomaterials 27 (2006) 3675–3683.
[6] J.P. Guyette, S.E. Gilpin, J.M. Charest, L.F. Tapias, X. Ren, H.C. Ott, Perfusion decellularization of whole organs, Nat. Protoc. 9 (2014) 1451–1468.
[7] J.A. DeQuach, S.H. Yuan, L.S.B. Goldstein, K.L. Christman, Decellularized porcine brain matrix for cell culture and tissue engineering scaffolds, Tissue Eng. Part A 17 (2011) 2583–2592.
[8] M.T. Wolf, K.A. Daly, E.P. Brennan-Pierce, S.A. Johnson, C.A. Carruthers, A. D'Amore, S.P. Nagarkar, S.S. Velankar, S.F. Badylak, A hydrogel derived from decellularized dermal extracellular matrix, Biomaterials 33 (2012) 7028–7038.
[9] A. D'Amore, T. Yoshizumi, S.K. Luketich, M.T. Wolf, X. Gu, M. Cammarata, R. Hoff, S.F. Badylak, W.R. Wagner, Bi-layered polyurethane – Extracellular matrix cardiac patch improves ischemic ventricular wall remodeling in a rat model, Biomaterials 107 (2016) 1–14.
[10] S. Baiguera, C. Del Gaudio, E. Lucatelli, E. Kuevda, M. Boieri, B. Mazzanti, A. Bianco, P. Macchiarini, Electrospun gelatin scaffolds incorporating rat decellularized brain extracellular matrix for neural tissue engineering, Biomaterials 35 (2014) 1205–1214.
[11] R. Inai, M. Kotaki, S. Ramakrishna, Structure and properties of electrospun PLLA single nanofibres, Nanotechnology 16 (2005) 208–213.
[12] S.Y. Gu, Q.L. Wu, J. Ren, G.J. Vancso, Mechanical properties of a single electrospun fiber and its structures, Macromol. Rapid Commun. 26 (2005) 716–720.

[13] V.J. Mase, J.R. Hsu, S.E. Wolf, J.C. Wenke, D.G. Baer, J. Owens, S.F. Badylak, T.J. Walters, Clinical application of an acellular biologic scaffold for surgical repair of a large, traumatic quadriceps femoris muscle defect, Orthopedics (2010).
[14] L. Huleihel, G.S. Hussey, J.D. Naranjo, L. Zhang, J.L. Dziki, N.J. Turner, D.B. Stolz, S.F. Badylak, Matrix-bound nanovesicles within ECM bioscaffolds, Sci. Adv. 2 (2016).
[15] B. Brown, K. Lindberg, J. Reing, D.B. Stolz, S.F. Badylak, The Basement membrane component of biologic scaffolds derived from extracellular matrix, Tissue Eng. 12 (2006).
[16] S.F. Badylak, D.O. Freytes, T.W. Gilbert, Extracellular matrix as a biological scaffold material: Structure and function, Acta Biomater. 5 (2009) 1–13.
[17] L.J. White, A.J. Taylor, D.M. Faulk, T.J. Keane, L.T. Saldin, J.E. Reing, I.T. Swinehart, N.J. Turner, B.D. Ratner, S.F. Badylak, The impact of detergents on the tissue decellularization process: a ToF-SIMS study, Acta Biomater. 50 (2017) 207–219.
[18] X. Li, Z. Li, L. Wang, G. Ma, F. Meng, R.H. Pritchard, E.L. Gill, Y. Liu, Y.Y.S. Huang, Low-voltage continuous electrospinning patterning, ACS Appl. Mater. Interfaces 8 (2016) 32120–32131.
[19] Z. Li, X. Li, Y.Y.S. Huang, Methods in Molecular Biology, Springer. (in press).
[20] E.H. Poppele, R.M. Hozalski, Micro-cantilever method for measuring the tensile strength of biofilms and microbial flocs, J. Microbiol. Methods 55 (2003) 607–615.
[21] N. Xue, X. Li, C. Bertulli, Z. Li, A. Patharagulpong, A. Sadok, Y.Y.S. Huang, Rapid patterning of 1-D collagenous topography as an ECM protein fibril platform for image cytometry, PLoS One 9 (2014).
[22] M.A. Saleem, M.J. O'Hare, J. Reiser, R.J. Coward, C.D. Inward, T. Farren, C.Y. Xing, L. Ni, P.W. Mathieson, P. Mundel, A conditionally immortalized human podocyte cell line demonstrating nephrin and podocin expression, J. Am. Soc. Nephrol. 13 (2002) 630–638.
[23] S.C. Satchell, C.H. Tasman, A. Singh, L. Ni, J. Geelen, C.J. Von Ruhland, M.J. O'Hare, M.A. Saleem, L.P. Van Den Heuvel, P.W. Mathieson, Conditionally immortalized human glomerular endothelial cells expressing fenestrations in response to VEGF, Kidney Int. 69 (2006) 1633–1640.
[24] C. Heckman, S. Kanagasundaram, M. Cayer, J. Paige, Preparation of cultured cells for scanning electron microscope, 2007.
[25] J.H. Song, H.E. Kim, H.W. Kim, Production of electrospun gelatin nanofiber by water-based co-solvent approach, J. Mater. Sci. Mater. Med. 19 (2008) 95–102.
[26] S. Heydarkhan-Hagvall, K. Schenke-Layland, A.P. Dhanasopon, F. Rofail, H. Smith, B.M. Wu, R. Shemin, R.E. Beygui, W.R. MacLellan, Three-dimensional electrospun ECM-based hybrid scaffolds for cardiovascular tissue engineering, Biomaterials 29 (2008) 2907–2914.
[27] Y. Zhang, H. Ouyang, T.L. Chwee, S. Ramakrishna, Z.M. Huang, Electrospinning of gelatin fibers and gelatin/PCL composite fibrous scaffolds, J. Biomed. Mater. Res. – Part B Appl. Biomater. 72 (2005) 156–165.
[28] P. Qi, Y. Zhou, D. Wang, Z. He, Z. Li, A new collagen solution with high concentration and collagen native structure perfectly preserved, RSC Adv. 5 (2015) 87180–87186.
[29] K. Gast, A. Siemer, D. Zirwer, G. Damaschun, Fluoroalcohol-induced structural changes of proteins: some aspects of cosolvent-protein interactions, Eur. Biophys. J. 30 (2001) 273–283.
[30] Merch Millipore, Safety data sheet for acetic acid (glacial) 100% 100063, 2017.
[31] Merch Millipore, Safety data sheet for ethyl acetate 100789, 2017.
[32] Merch Millipore, Safety data sheet for 1,1,1,3,3,3-Hexafluoro-2-propanol 845157, 2017.
[33] R.K. Assoian, A. Komoriya, C.A. Meyers, D.M. Miller, M.B. Sporn, Transforming growth factor-beta in human platelets. Identification of a major storage site, purification, and characterization, J. Biol. Chem. 258 (1983) 7155–7160.
[34] T.K. Sampath, A.H. Reddi, Homology of bone-inductive proteins from human, monkey, bovine, and rat extracellular matrix, Proc. Natl. Acad. Sci. U.S.A. 80 (1983) 6591–6595.
[35] J.P. López-Alonso, M. Bruix, J. Font, M. Ribó, M. Vilanova, M.A. Jiménez, J. Santoro, C. González, D.V. Laurents, NMR spectroscopy reveals that RNase A is chiefly denatured in 40% acetic acid: Implications for oligomer formation by 3D domain swapping, J. Am. Chem. Soc. 132 (2010) 1621–1630.
[36] E. Hemaprabha, Chemical crosslinking of proteins: a review, J. Pharm. Sci. Innov. 1 (2012) 22–26.
[37] C. Marquié, Chemical reactions in cottonseed protein cross-linking by formaldehyde, glutaraldehyde, and glyoxal for the formation of protein films with enhanced mechanical properties, J. Agric. Food Chem. 49 (2001) 4676–4681.
[38] O. Sids, U. Publications, Introduction Glyoxal Cas N° : 107-22-2, (n.d.).
[39] O. Sids, U. Publications, Formaldehy De, Unep Publ. (2002) 1–395.
[40] Organisation for Economic Co-Operation and Development Screening Information Data Sets (OECD SIDS), Glutaradehyde CAS N°: 111-30-8, UNEP Publ. (2008) 1–83.
[41] P. Davis, B.E. Tabor, Kinetic study of the crosslinking of gelatin by formaldehyde and glyoxal, J. Polym. Sci. Part A Gen. Pap. 1 (1963) 799–815.
[42] B.H. Stuart, D.J. Ando, Biological Applications of Infrared Spectroscopy, 1997.
[43] R.J. Pelham, Y.L. Wang, Cell locomotion and focal adhesions are regulated by the mechanical properties of the substrate, Biol. Bull. (1998) 348–350.
[44] A.J. Engler, S. Sen, H.L. Sweeney, D.E. Discher, Matrix elasticity directs stem cell lineage specification, Cell 126 (2006) 677–689.
[45] V.Z. Beachley, M.T. Wolf, K. Sadtler, S.S. Manda, H. Jacobs, M.R. Blatchley, J.S. Bader, A. Pandey, D. Pardoll, J.H. Elisseeff, Tissue matrix arrays for high-throughput screening and systems analysis of cell function, Nat. Methods 12 (2015) 1197–1204.
[46] Y.Y.S. Huang, E.M. Terentjev, T. Oppenheim, S.P. Lacour, M.E. Welland, Fabrication and electromechanical characterization of near-field electrospun composite fibers, Nanotechnology 23 (2012) 105305.
[47] D.J. Rosario, G.C. Reilly, E.A. Salah, M. Glover, A.J. Bullock, S. MacNeil, Decellularization and sterilization of porcine urinary bladder matrix for tissue engineering in the lower urinary tract, Regen. Med. 3 (2008) 145–156.
[48] W.A. Farhat, J. Chen, J. Haig, R. Antoon, J. Litman, C. Sherman, K. Derwin, H. Yeger, Porcine bladder acellular matrix (ACM): protein expression, mechanical properties, Biomed. Mater. 3 (2008) 25015.
[49] R. Middleton, X. Li, J. Shepherd, Z. Li, W. Wang, S.M. Best, R.E. Cameron, Y.Y.S. Huang, Near-field electrospinning patterning polycaprolactone and polycaprolactone/collagen interconnected fiber membrane, Macromol. Mater. Eng. 303 (2018) 1700463.
[50] S.M. Park, D.S. Kim, Electrolyte-assisted electrospinning for a self-assembled, free-standing nanofiber membrane on a curved surface, Adv. Mater. 27 (2015) 1682–1687.
[51] S. Kusuma, S. Zhao, S. Gerecht, The extracellular matrix is a novel attribute of endothelial progenitors and of hypoxic mature endothelial cells, FASEB J. 26 (2012) 4925–4936.
[52] S.C. Slater, V. Beachley, T. Hayes, D. Zhang, G.I. Welsh, M.A. Saleem, P.W. Mathieson, X. Wen, B. Su, S.C. Satchell, An in vitro model of the glomerular capillary wall using electrospun collagen nanofibres in a bioartificial composite basement membrane, PLoS One 6 (2011) e20802.
[53] S. Slater, V. Beachley, X. Wen, T. Hayes, B. Su, M. Saleem, P. Mathieson, S. Satchell, Development of a functional model of the glomerular filtration barrier using electrospun collagen nanofibres in a bioartificial composite basement membrane, Eur. Cells Mater. 18 (2009) 39.

Supporting Information

Solution Fibre Spinning Technique for the Fabrication of Tuneable Decellularised Matrix-Laden Fibres and Fibrous Micromembrane

Zhaoying Li[a,b], Jack Tuffin[c], Iek M. Lei[a,b], Francesco S. Ruggeri[d], Natasha S. Lewis[a,b], Elisabeth L. Gill[a,b], Thierry Savin[a], Luai Huleihel[e], Stephen F. Badylak[e], Tuomas Knowles[d,f], Simon C. Satchell[c], Gavin I. Welsh[c], Moin A. Saleem[c] and Yan Yan Shery Huang*[a,b]

[a] Department of Engineering, University of Cambridge, Cambridge CB2 1PZ, UK
[b] The Nanoscience Centre, University of Cambridge, Cambridge CB3 0FF, UK
[c] Bristol Medical School: Translational Health Sciences, University of Bristol, Bristol BS1 3NY, UK
[d] Department of Chemistry, University of Cambridge, Cambridge CB2 1EW, UK
[e] McGowan Institute for Regenerative Medicine, Pittsburgh, PA 15219, USA
[f] Cavendish Laboratory, University of Cambridge, Cambridge, CB3 1HE, UK
*Email: yysh2@cam.ac.uk

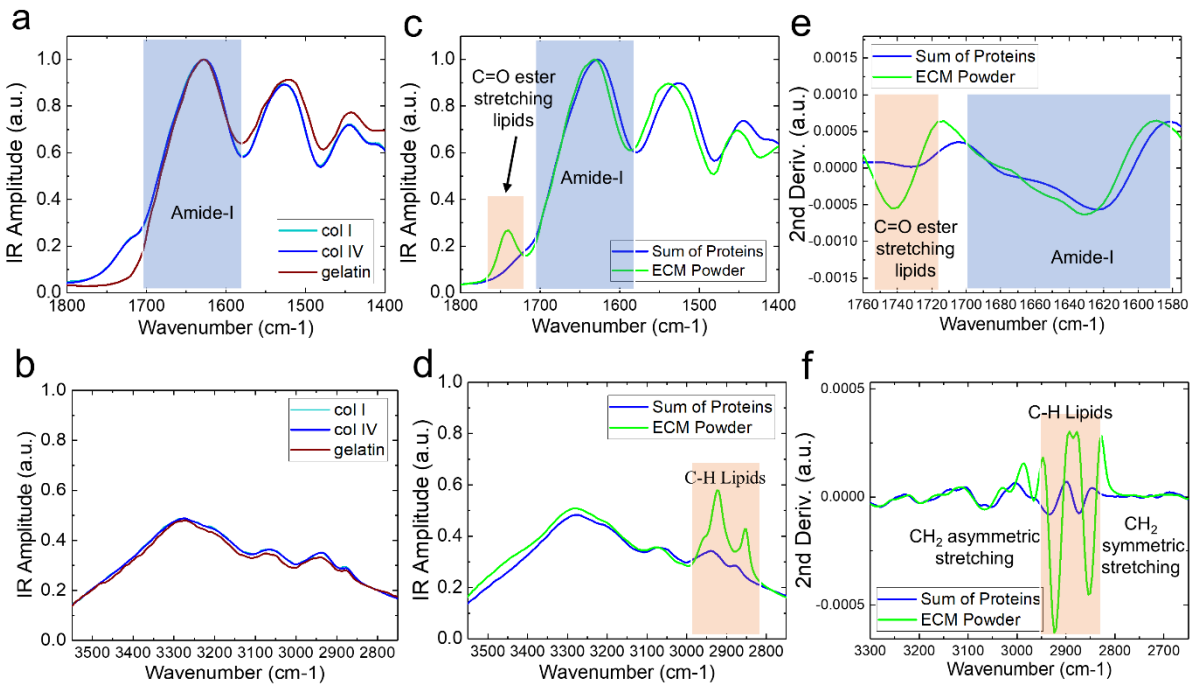

Figure S1: FTIR spectra of reference proteins and the ECM powder. (a – b) Spectra of individual reference proteins (collagen I, collagen IV and gelatin) showing the presences of amide-I (1580 – 1700 cm^{-1}) and amide-II (1520 – 1580 cm^{-1}) bands; (c – d) Spectra of the ECM power and the normalised sum of reference proteins; (e – f) Second derivative analysis of the spectra.

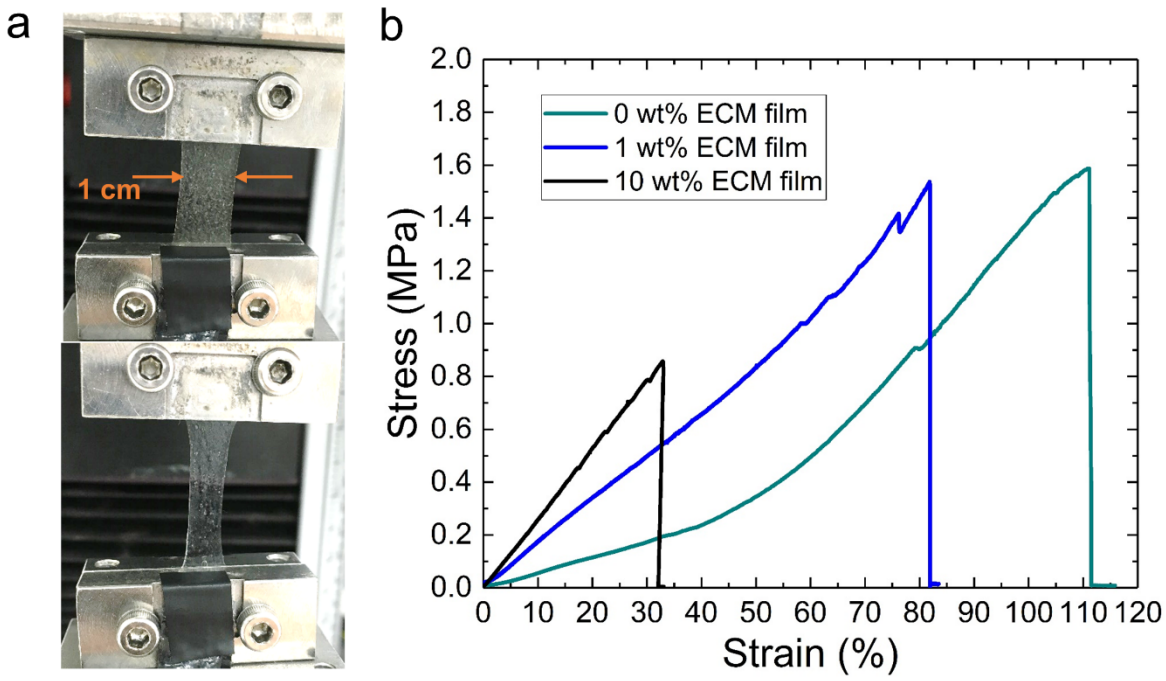

Figure S2: (a) Reference films were installed on Instron 5544 and deformed at a rate of 0.6mm/min. Young's moduli of the films were then calculated based on the deformation measurements; (b) Stress – strain curves of reference films with different ECM compositions. Young's moduli of films increased with the composition of ECM.

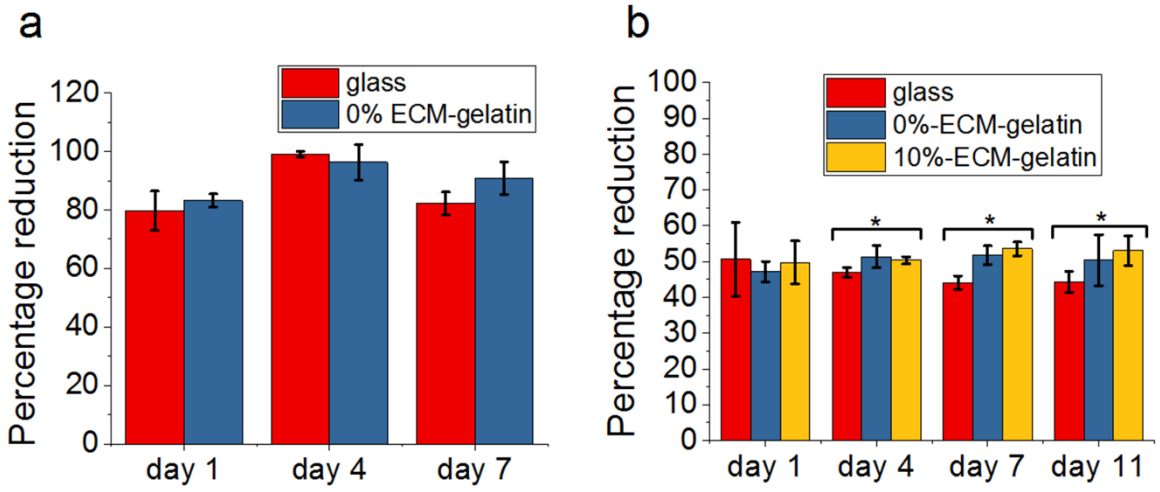

Figure S3: Percentage reduction (± 95% confidence interval) of alamarBlue by (a) EA.hy926 cells cultured on a glass control substrate and pure gelatin fibres, and (b) podocytes cultured on glass control, pure gelatin fibres, and 10 wt% ECM fibres. High percentage reduction indicates high cellular activity. Statistical significance was evaluated using a Mann-Whitney U test (a) and a Kruskal-Wallis test (b). *$p < 0.05$.

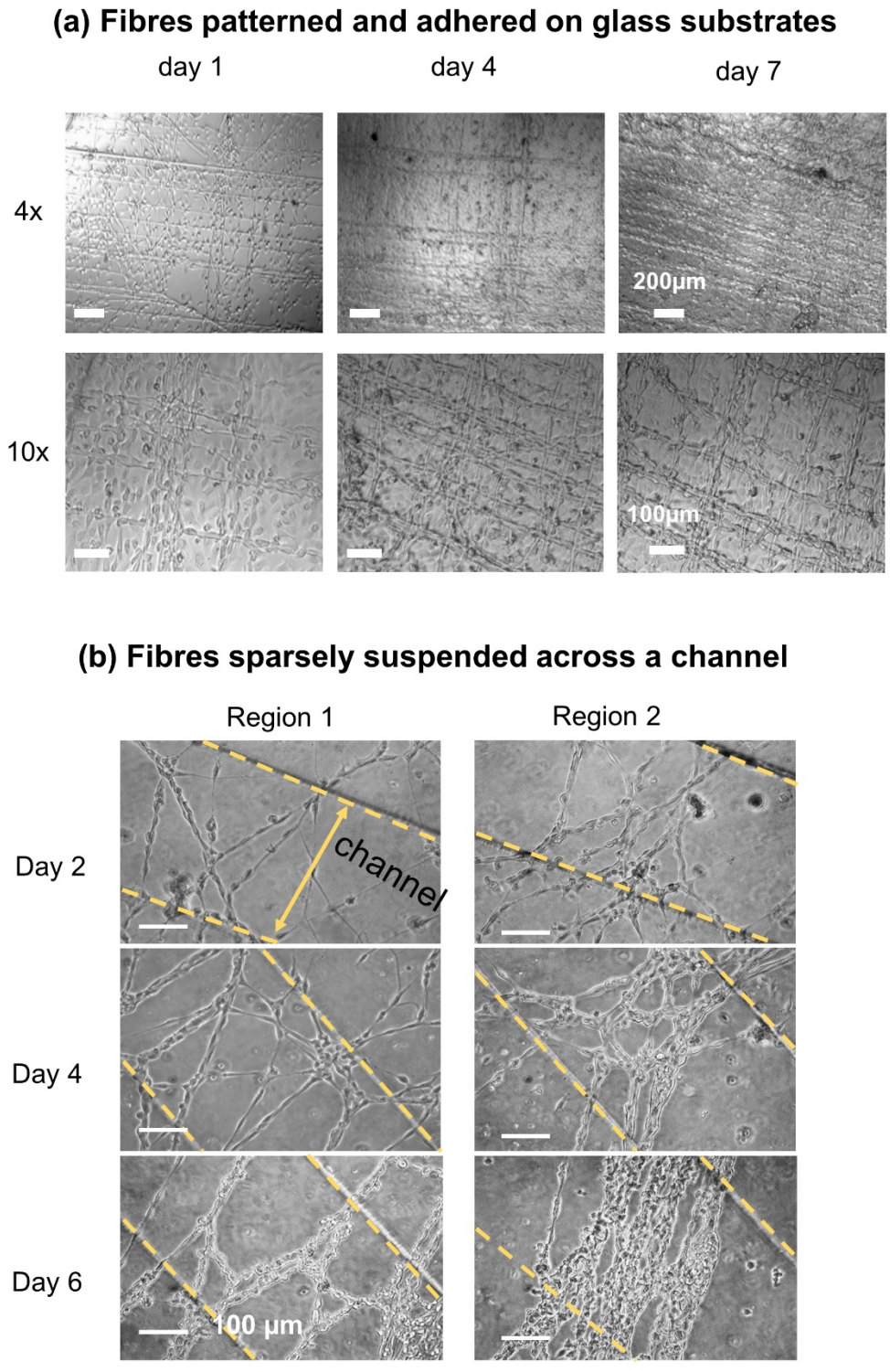

Figure S4: (a) EA.hy926 cells cultured on pure gelatin fibre-glass substrates, showing optical images acquired at different time points at two magnifications. (b) EA.hy926 cells cultured on pure gelatin fibres sparsely suspended over a channel, showing optical images acquired at different time points at two different regions.

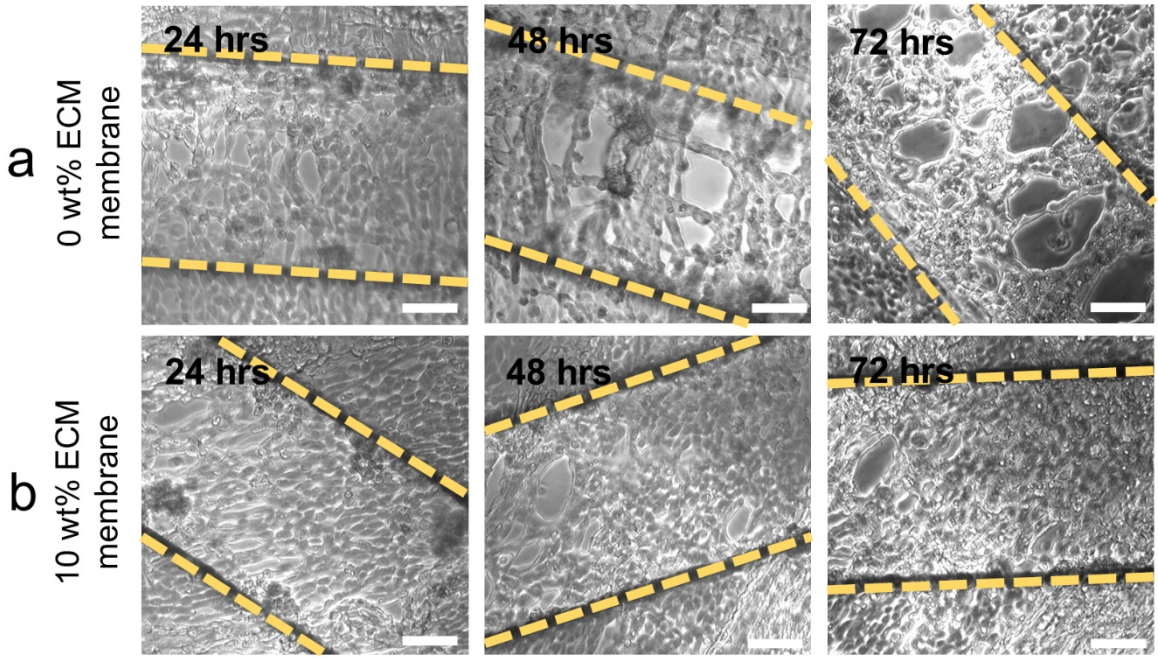

Figure S5: Remodelling of fibrous membrane with dense mesh by EAhy926 cells. (a) EA.hy926 cells cultured on a 0 wt% ECM membrane for differen time points. A cord-like network formed eventually and mesh size was enlarged over time; (b) EA.hy926 cells cultured on a 10 wt% ECM membrane for different time points. Membrane geometry remained roughly unchanged. Scale bar 50 µm.

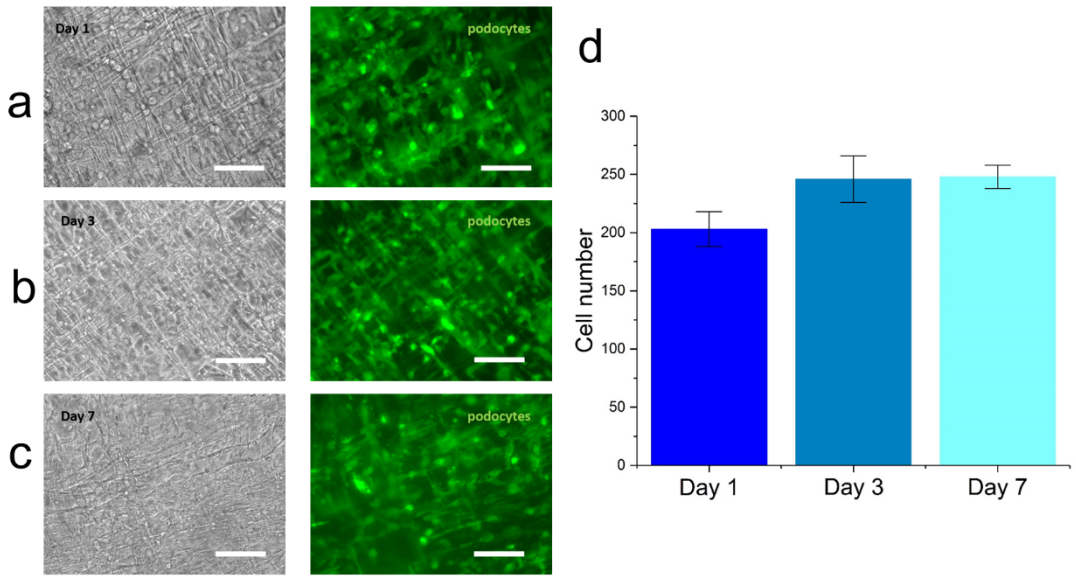

Figure S6: Optical micrographs and confocal images showing co-culture of GEnCs and podocytes on a suspended 10 wt% ECM membrane for (a) 1 day, (b) 3 days and (c) 7 days. Membrane structure was retained, and cells remained attached to membrane after 7 days of culturing. Scale bar 50 μm; (d) Number of cells counted in the area of imaging (200 x 150 μm^2).

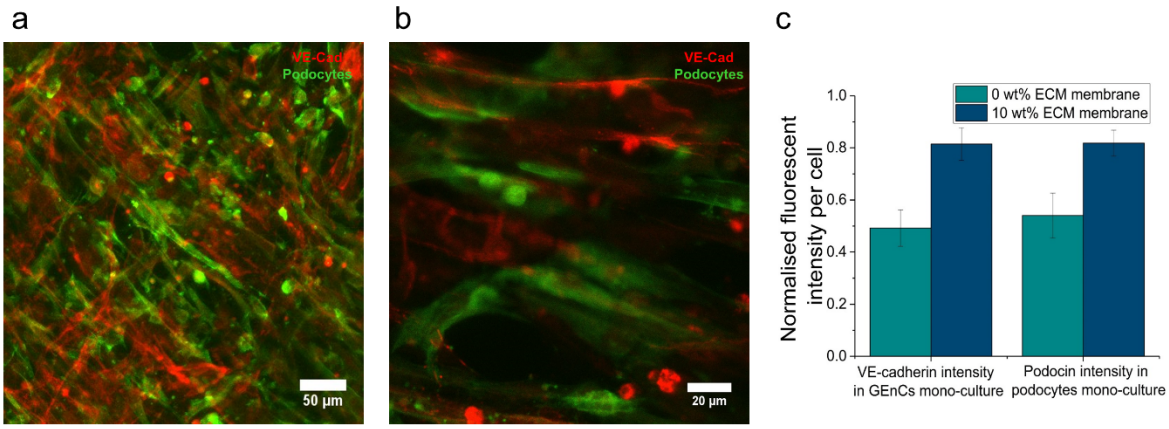

Figure S7: Co-culture of GEnCs and podocytes on (a) a 0 wt% ECM membrane and (b) a 10wt% ECM membrane. (c) Normalised fluorescent intensity per cell of VE-Cadherin in GEnCs mono-culture, and podocin in podocytes mono-culture, n=3. Each sample contained 50 – 60 cells.